Trace detection of pyridine based on HCPCF SERS sensor

Di Zhigang[1], Wang Biao[1], Yang Jiantan[1], Jia Chunrong[1], Zhang Jingxuan[1], Yao Jianquan[2], Lu Ying[2]

(1. College of Electrical Engineering, North China University of Science and Technology, Tangshan 063210, China;
2. Key Lab of Opto-electronics Information Science and Technology, Ministry of Education, College of Precision Instrument and Optoelectronics Engineering, Tianjin University, Tianjin 300072, China)

Abstract: "Food is the paramount necessity of the people, safety is the first concern for the food", under the background of widespread application of various pesticides and food additives, illegal food additives have a serious impact on the food safety situation, and the qualitative detection of trace amounts of illegal food additives is of great significance. In order to achieve qualitative detection of pyridine, a sensing system based on HCPCF (Hollow Core Photonic Crystal Fiber) SERS was proposed. Silver nanoparticles were used to make SERS substrate, and SERS signal devices were designed to collect SERS in the same direction. By means of cone pulling on HCPCF to achieve selective filling, the detection scheme of collecting output signals by spectrometer was implemented. After the liquid pyridine sample with the concentration of 0.004 975% was detected, the obvious SERS characteristic spectrum could be observed. The experimental results show that the sensing system can achieve qualitative trace detection of pyridine in the liquid sample.

Key words: food safety; photonic crystal fiber sensing; nanoparticle; SERS; trace detection

CLC number: TN253 **Document code:** A **DOI:** 10.3788/IRLA201948.S213004

基于 HCPCF SERS 传感器的吡啶痕量检测

邸志刚[1],王 彪[1],杨健倓[1],贾春荣[1],张靖轩[1],姚建铨[2],陆 颖[2]

(1. 华北理工大学 电气工程学院,河北 唐山 063210;
2. 天津大学 精密仪器与光电工程学院 教育部光电信息科学与技术重点实验室,天津 300072)

摘 要: “民以食为天,食以安为先”,在各种农药,食品添加剂广泛应用的背景下,非法食品添加剂对食品安全形势造成严重影响,非法食品添加剂痕量定性检测有重大意义。为实现对吡啶的定性检测,提出了一种基于 HCPCF(Hollow Core Photonic Crystal Fiber)SERS 的传感系统,采用银纳米颗粒制作 SERS 基底,设计同向收集 SERS 信号装置,通过对 HCPCF 拉锥并实现选择性填充,利用光谱仪采集输出信号的检测方案。经对浓度为 0.004 975%的液体样本进行试验, 检测出明显的吡啶特征 SERS 谱。实验结果表明该传感系统能够实现对液体样本中吡啶痕量的定性检测。

关键词: 食品安全; 光子晶体光纤传感; 纳米颗粒; SERS; 痕量检测

收稿日期: 2019-04-01; **修订日期:** 2019-05-14

基金项目: 国家 973 计划(2010CB327801);河北省食品药品监督管理局科技计划重点项目(ZD201516);
河北省高等学校科学技术研究项目(QN2016079);华北理工大学培育基金(SP201502)

作者简介: 邸志刚(1975-),男,副教授,博士,主要从事光子晶体光纤传感方面的研究。Email:dzg0512@126.com

导师简介: 姚建铨(1939-),男,中国科学院院士,教授,主要从事光电子技术、物理电子学、非线性光学等方面的研究。
Email:jqyao@tju.edu.cn

0 Introduction

As an important chemical raw material and excellent solvent and coloring agent, pyridine is widely applied. But its physical and chemical properties have great harm on health and environment[1], and the wrong storage and transportation methods have great safety hazards. The current main pyridine detection methods are barbituric acid spectrophotometry[2] and headspace gas chromatography[3]. Headspace gas chromatography is mainly suitable for the analysis of waste water. Barbituric acid spectrophotometry requires the use of highly toxic potassium cyanide. The pretreatment is cumbersome and has low sensitivity. With the development of science and technology, many new materials and technologies have come into people′s life frequently, such as the fiber SERS sensor combined with low loss fiber and SERS, which has been widely used in many fields[4-5], and apply nanomaterials in optics and electromagnetism[6-7], as well as HCPCF with unique properties. The current fiber-optic SERS sensor has the disadvantage that the number of base particles in the active region is small, and a higher laser intensity or longer time is required to obtain an ideal SERS spectrum, so it cannot be used widely. But the new HCPCF SERS sensor, which is composed of HCPCF and SERS sensors, has been paid more attention in the field of chemical, biological and environmental detection[8]. For these reasons, this paper used HCPCF SERS sensing technology to detect trace amounts of illegal food additive pyridine.

1 Experimental scheme

The HCPCF SERS sensor was proposed to detect trace amounts of illegal food additive pyridine. The HCPCF SERS sensing system is combined by HCPCF and SERS sensors, and can detect the trace qualitative of liquid samples. The experiment test object was the trace pyridine in the sample solution.

1.1 Experimental principle

The principle of this experimental protocol is the combination of SERS sensing and HCPCF sensing. According to the actual requirements, the experimental scheme of collecting SERS signals in the same direction is designed. The experimental principle was shown in Fig.1.

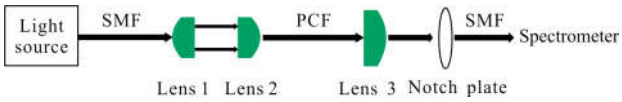

Fig.1 Experimental principle diagram of co-direction acquisition

First, the suitable SERS substrate was manufactured in the prepared HCPCF air hole, second, the liquid sample were injected into the air hole of HCPCF, and then the excitation light of 785 nm was coupled into the HCPCF to excite the SERS signal. Finally, the generated SERS signal was detected by a spectrometer.

In Fig.1, the excitation light output by the light source is collimated into the HCPCF to excite the SERS signal by the lens 1 and lens 2, and then the SERS signal is collected by the lens 3 in the same direction. Because the excitation light signal is mixed in the SERS signal, the excitation light is filtered through a notch plate. The experimental protocol for this configuration is suitable for trace detecting in liquid samples.

1.2 Main equipment

The instruments used in the experiment include light source, lens, notch plate and spectrometer, which are described separately as follows.

1.2.1 Light source

In the Raman spectroscopy test, the commonly used excitation wavelengths are 514, 633, 785, 1 064 nm. The light source used in this experiment is FCD-785A semiconductor laser purchased from Changchun New Industry Opto-electronics Co., LTD. The output power of optical fiber is 300 mW and the stability is within 3%.

1.2.2 Laser notch plate

When the SERS signal was collected in the

experiment, the excitation light would have a great influence, so the 785 nm light was filtered out by a laser notch plate, which was produced by Semrock, USA, the notch bandwidth is 39 nm.

1.2.3 Spectrometers

WGD -4B composite multifunctional grating spectrometer was used for the spectrometer. The wavelength range was 4 000-650 cm^{-1}, the focal length was 300 mm, the wavelength precision was 4 cm^{-1}, the wavelength repeatability was 1 cm^{-1}, and the resolution was 6 absorption peaks of polystyrene.

Agilent 86142B spectrometer, with wavelength accuracy of 10 PM, test range of 600 -1 700 nm, sensitivity of 90 dBm and bandwidth range of 0.2 nm to full range was utilized in this research. This spectrometer is suitable for system testing which requires very strict precision of power and wavelength.

1.3 Research on HCPCF simulation

1.3.1 HCPCF COMSOL simulation

In this paper, HCPCF with the structure of Fig.2 is built by COMSOL software RF module[9]. The red

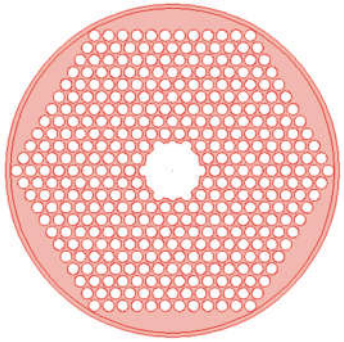

Fig.2 Structural schematic diagram of HCPCF

part is made of silicon, the white part is made of air, the perfect matching layer of the outer ring is set to absorb completely in the X and Y directions in the rectangular coordinate system, the inner boundary is set to be continuous, the outer boundary is set to be a perfect magnetic conductor, the free space wavelength is set in the application mode parameters, and the wavelength is set to 785e^{-9} in the application scalar variables. Specific structural parameters are silicon refractive index 1.45, air refractive index 1.0, cladding air hole radius r_{clad}=0.65 μm, hole spacing Λ=1.65 μm, core air hole radius r_{core}=3.2 μm, air filling ratio $f=\frac{\pi}{2\sqrt{3}}\frac{4r_{clad}^2}{\Lambda^2}=56.30\%$.

By setting the initial value of the calculation, the effective refractive index range is set to 0.996, and find 20 solutions. It can be calculated that the electric field energy and distribution are shown in Fig.3 (a) and 3(b).

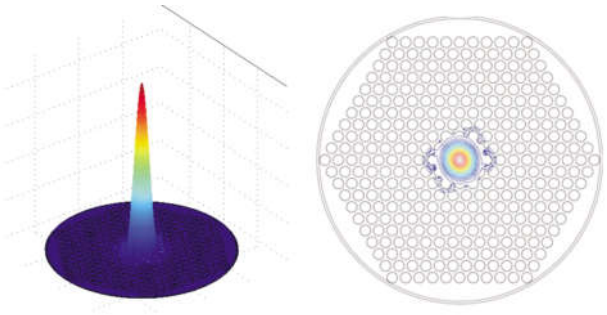

(a) Three-dimensional distribution diagram (b) Equipotential distribution diagram

Fig.3 Electric field normalization

By post process, n_{eff} is 3.298×10^{-12}, the confinement loss is 0.32 dB/m.

1.3.2 Numerical simulation of HCPCF silver plated nanofilm

A silver nano-film with a diameter of 78 nm is plated into the core of the HCPCF, and the structure is shown in Fig.4.

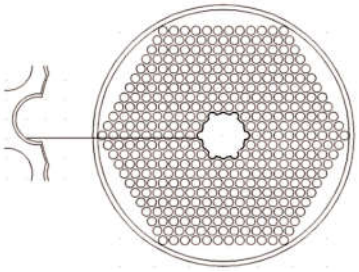

Fig.4 Structural sketch of silver-plated nano-films on HCPCF core holes

After COMSOL simulation, the HCPCF field distribution of 78 nm thick silver nanofilm is shown in Fig.5.

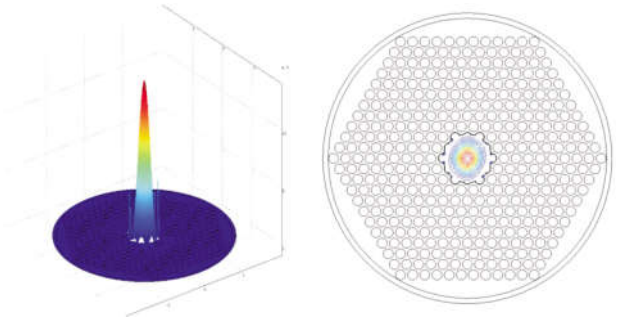

(a) Three-dimensional field distribution (b) Equipotential field distribution

Fig.5 Simulation results of HCPCF silver-plated nanofilm

It can be seen from the figure that the silver-plated nano-film can better restrict the transmission of light in the core, which is conducive to better SERS effect. And its confinement loss is 0.41 dB/m.

1.3.3 Numerical simulation of liquid filled HCPCF silver-plated nanofilm COMSOL

Since PCF SERS sensing is generally used for detecting liquid samples, that is, when HCPCF is directly immersed into the sample solution to be tested, the air holes of fiber core and cladding will be filled with liquid, so it is necessary to simulate and calculate the coating HCPCF for filling liquid. HCPCF is filled with liquid in two ways. One is that the liquid is filled with only the air hole of the fiber core; the other is that both the fiber core and the air hole of the cladding are filled with liquid. In this part, the simulation calculation is carried out for the two cases. HCPCF mentioned above is adopted, and 78 nm thick silver nanometer film coating is carried out for the air hole of fiber core. The simulation results are as follows.

Only the air hole of the fiber core is filled with liquid, namely the liquid core HCPCF, and its field distribution is shown in Fig.6, and its confinement loss is 0.30 dB/m.

The fiber core and cladding air hole are filled with liquid, namely the whole liquid HCPCF. The field distribution is shown in Fig.7.

Comparing Fig.6 and Fig.7, it can be seen that the liquid core HCPCF has a much better ability to limit light. By calculation, its confinement loss is 0.43 dB/m, which is bigger because more light excite Raman scattering effect.

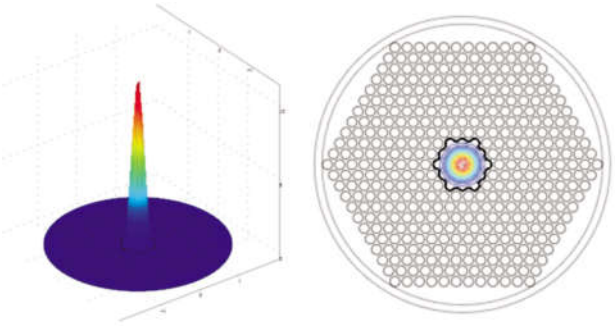

(a) Three-dimensional field distribution diagram (b) Equipotential field distribution map

Fig.6 Simulation results of silver-plated nanometer film HCPCF in liquid core

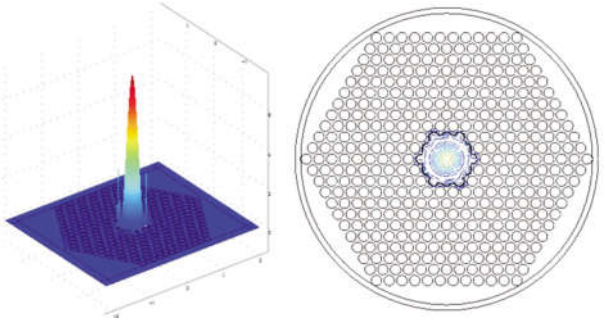

(a) Three-dimensional field distribution diagram (b) Equipotential field distribution map

Fig.7 Simulation results of full-liquid silver coated nanometer film HCPCF

By the comparison above, the liquid core HCPCF was more suitable for SERS sensor, so it was used in this experiment.

1.4 Experimental preparation

During the experiment, the target of detection was a low concentration of pyridine in aqueous solution.

1.4.1 HCPCF

Due to the fact that the HCPCF could not be obtained as described above, this experiment used the Air-6-800 with similar structure and relatively easy to obtain. The HCPCF is produced by Crystal Fiber of

Denmark and can be tested at an excitation wavelength of 785 nm. The structural parameters of this fiber are shown in Tab.1. Its structure diagram and transmission line are shown in Fig.8.

Tab.1 Air-6-800 technical parameters

Material	Pure silicon
Outer layer diameter/μm	122±5
Coating diameter/μm	243±10
Core hole diameter/μm	6±1
Cladding hole diameter/μm	1.3
Hole spacing/μm	1.65
Transmission bandwidth/nm	60

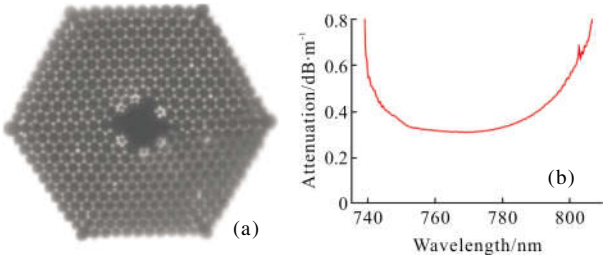

Fig.8 Air-6-800 HCPCF (a) block diagram (b) attenuation vs wavelength

The Air-6-800 was numerically simulated with COMSOL software in the same manner as described above. After simulation calculation, the effective refractive index is $0.995\,814-i1.256\,822e^{-9}$, and its field distribution was shown in Fig.9.

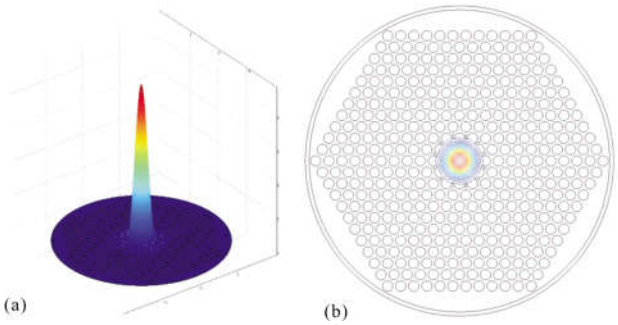

Fig.9 Air-6-800 (a) three-dimensional (b) equipotential field distribution

Since the experimental object is a certain concentration of strontium sample solution, according to the previous simulation results, the liquid core HCPCF light-limited ability is stronger, by understanding the Cristiano MB Cordeiro research group[10] and Stephan Smolka[11] respectively related to selective filling. In the experiment, this paper adopts a selective filling scheme, which uses the taper function of the fiber fusion splicer to collapse the cladding air hole of the HCPCF and keep the core hole unchanged, thus achieving selective filling. The specific implementation process is as follows. First, the HCPCF is cut into 5 cm segments, then the coating layer in the middle part of each HCPCF is removed. Then the fiber fusion splicer (Ericsson FSU-925) is used to pull the cone. When drawing the cone, pay attention to the HCPCF collimation on the same level, as shown in Fig.10.

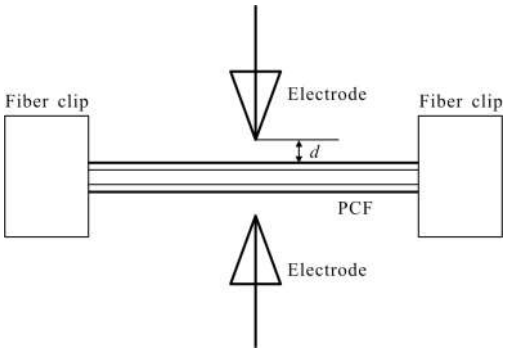

Fig.10 Pull the cone with fiber fusion splicer

When the taper is drawn, only the cladding holes collapse and the core remains intact. It depends entirely on the discharge current, the tension and the heat transfer effect of the material[12]. It is necessary to set the distanced between the electrode and HCPCF, the discharge time and the discharge current[13]. The current between electrodes can be expressed as:

$$i(r,z)=\frac{I_0}{2\pi\sigma^2(z)}\exp\left(-\frac{r^2}{2\sigma^2(z)}\right) \tag{1}$$

$$\sigma(z)=\sigma_0(1+z^2)^{-1/3} \tag{2}$$

Where I_0 is the total current obtained by integrating the entire r, σ (z) is the Gaussian width at z, and σ_0 is the Gaussian width at the point z=0 in the electrode. Space temperature is proportional to current density, which is

$$T(r,z)\propto i^2(r,z) \tag{3}$$

The temperature distribution diagram is shown in Fig.11.

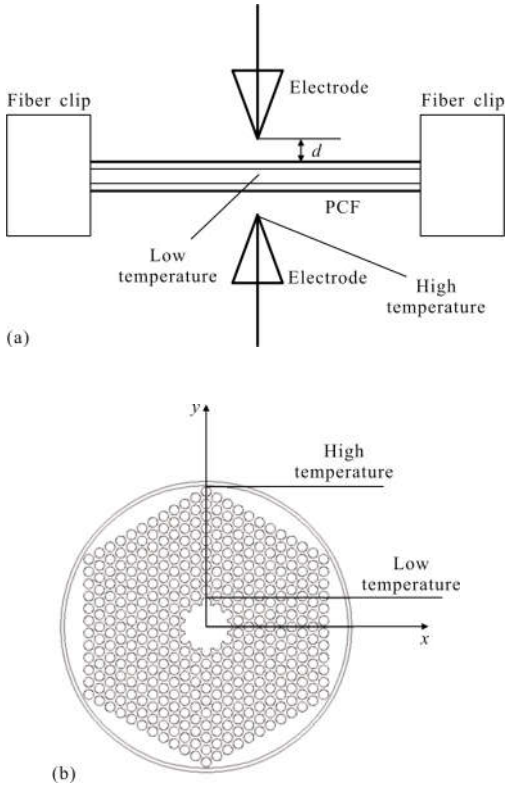

Fig.11 Distribution of the space temperature of the HCPCF

It can be seen from Fig.11 that the temperature at the tip of the electrode is highest, and it is also found that the temperature at the surface of the HCPCF is the highest and the temperature at the core is the lowest. The thermal conductivity of solid silicon in HCPCF is gradually reduced from the cladding to the core due to the presence of air. And when the heating rate is

$$V_{\text{collapse}}=\frac{\gamma}{2\eta(T)} \tag{4}$$

The cladding hole will collapse. In Eq.(4), γ is the surface tension and η is the viscosity of silicon. Since the viscosity drops rapidly with increasing temperature, the air holes in the high temperature region collapse faster, causing the cladding air holes of the HCPCF to collapse before the core holes. If the appropriate taper parameters are selected, the HCPCF cladding air hole collapses and the core air holes remain intact.

For Ericsson FSU-925, after parameter adjustment, when the spacing d=0 μm, discharge time 400 ms, discharge current 11 mA, the taper effect is the best, and its effect diagram is shown in Fig.12.

Fig.12 HCPCF taper effect diagram

After the taper, the HCPCF was taken out and cut into two sections from the middle with a cutter to carry on the experiment. The effect diagram after cutting is shown in Fig.13.

Fig.13 Effect diagram after HCPCF taper cutting

After the above treatment, HCPCF can achieve selective filling, that is, only the liquid sample is immersed into the core air hole, while the cladding hole is still air.

1.4.2 SERS substrate preparation

At present, there are various methods for preparing SERS substrates[14-15]. In order to facilitate the control of nanoparticles, considering the advantages and disadvantages of various methods, the SERS substrate is prepared by suspending silver nanoparticles.

By research before, the Ag nanoparticles with a diameter of 78 nm had better SERS effect[16], so they were utilized in this experiment, which were purchased from Xuzhou Jet Innovative Materials Technology Co., Ltd. The silver nanoparticles were precipitated in the sample solution during the initial preparation, so that the silver nanoparticles could not be uniformly suspended. The silver nanoparticles can be suspended in liquid by adding surfactant properly. In the later experimental preparation, CTAB(cetyltrimethy

lammonium bromide) was dissolved in the sample solution, and the silver nanoparticles were suspended uniformly instead of precipitating, as shown in Fig.14.

Fig.14 Effect of silver nanoparticles suspended in the liquid to be tested

By controlling the concentration of silver nanoparticles in solution to change the distance between silver nanoparticles, SERS signal can be more effectively activated. In addition, the size of silver nanoparticles in optical fibers is also controlled. But this method can only judge its specific effect by testing samples.

1.4.3 Solution preparation

For pyridine solution, attention must be paid to avoid sunlight exposure. This experiment was performed in a cleanroom laboratory and configured in a glass. The purchased pyridine concentration was 99.5%, and 1 mL of the solution was prepared at the time of preparation, and it was placed in 1 000 mL of distilled water to obtain a pyridine solution with a concentration of 0.099 5%. Then, three parts of 10 mL solution were placed in 100, 200, 500 mL distilled water, and pyridine solutions with concentrations of 0.009 995%, 0.004 975%, and 0.001 99% were obtained.

78 nm of silver nanoparticles were placed in the prepared liquid to be tested to produce an enhanced Raman signal. In order to uniformly suspend the silver nanoparticles in the liquid to be tested, it is necessary to add a surfactant, CTAB (cetyltrimethy lammonium bromide), into the liquid.

1.4.4 Liquid sample injection

Since the core hole of the PCF is relatively thin, it is difficult to inject the liquid. Claire Gu et al [17] used siphoning to inject, but the inhalation was slower. In this paper, a syringe is used to inject the liquid to be tested, as shown in Fig.15.

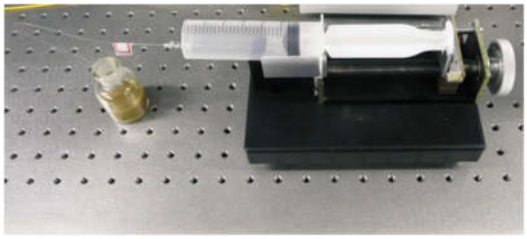

Fig.15 Diagram of PCF liquid sample injection device

2 Experiment results and analysis

By the preparations above, the pyridine solution sample can be tested. The physical picture of the experiment is shown in Fig.16.

Fig.16 Physical diagram of PCF SERS sensing system

Firstly, the performance of the light source was tested. The output laser of the light source was coupled into Air-6-800 by an adapter, and its output power was measured at about 150 micron. The waveform measured by Agilent 86142B spectrometer was shown in Fig.17.

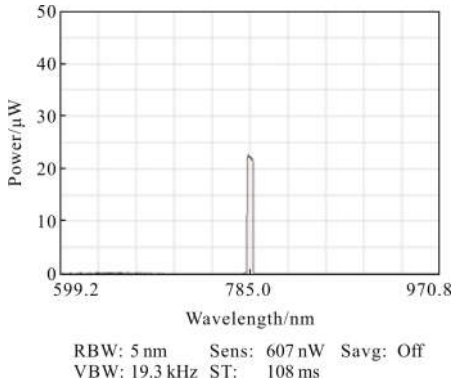

Fig.17 Output spectrum after the source is coupled into the HCPCF

The prepared pyridine solution was tested by a built-up experimental system.The experiment was done in clean room, and first the background was shown in Fig.18.

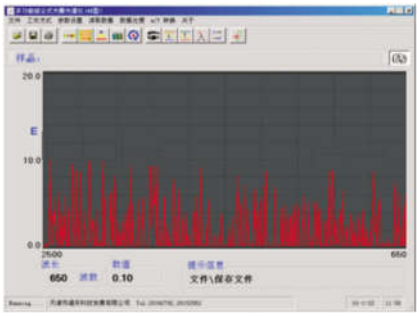

Fig.18 Background of SERS spectrum

When the pyridine solutions with concentrations of 0.009 995%, 0.004 975%, and 0.001 99% were detected, only solutions with concentrations of 0.009 995%, 0.004 975% could obtain a distinct characteristic spectrum, the SERS spectrum of solution with concentration of 0.004 975% was shown in Fig.19. When the background light was subtracted, the SERS spectrum was shown in Fig.20.

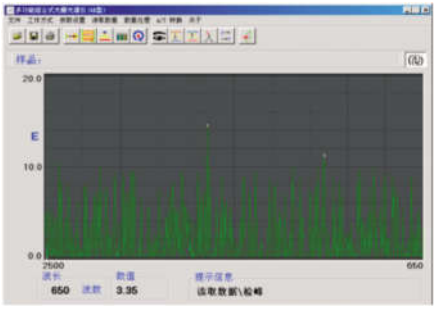

Fig.19 Pyridine SERS spectrum

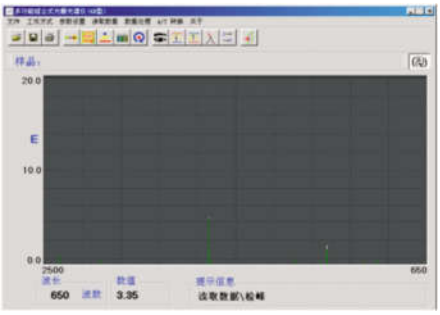

Fig.20 Pyridine SERS spectrum

As can be seen from Fig.20, for this concentration of pyridine solution, there are characteristic peaks at 1 068 cm^{-1} and 1 544 cm^{-1}, and the results are basically consistent with the results of Richard L. McCreery[18], thereby demonstrating the presence of pyridine.

3 Conclusion

The PCF SERS sensor was researched in this paper. First, by COMSOL simulation we designed suitable HCPCF, and by drawing the cone on HCPCF and selective filling, the liquid core PCF was obtained. Second, by filling Ag nanoparticles in HCPCF, the SERS substrate was manufactured. Then liquid core HCPCF was combined with SERS substrate, the HCPCF SERS sensor was acquired. Finally it was applied in trace detection of pyridine solution in food additives, and concentration detection limitation can reach 0.004 975%. As a result, we can draw a conclusion that HCPCF SERS sensor can be utilized in food safety detection.

References:

[1] Wang Hongli, Liu Suli, Zhao Mei, et al. Research progress on the harm of illegal addition of industrial dyes in food[J]. ***Journal of Food Safety and Quality***, 2019, 10(1): 1-7.

[2] The Ministry of Health of the P.R. China, Standardization Administration of the P.R. China. GB5749-2006. Standards for drinking water quality, the national standard of the P.R. China [S]. Beijing: China Standard Press, 2007: 2-4. (in Chinese)

[3] National Environmental Protection Agency, The State Bureau of Technical Supervision. GB 15618-1993. Water quality-determination of pyridine-gas chromatography [S]. Beijing: China Standards Press, 1993.

[4] Geng Y, Xu Y, Tan X, et al. A simplified hollow-core photonic crystal fiber SERS probe with a fully filled photoreduction pilver nanoprism [J]. ***Sensors***, 2018, 18(6): 1726.

[5] Zhang L, Li J S. Design and measurement of all-rod terahertz photonic crystal fiber with air-core [J]. ***Optics Communications***, 2015, 344: 77-80.

[6] Wang Q, Song F, Lin S, et al. Optical properties of silver nanoprisms and their influences on fluorescence of europium

complex[J]. ***Optics Express***, 2011, 19(8): 6999.

[7] Cheng Ziqiang, Shi Haiquan, Yu Ping, et al. Surface-enhanced Raman scattering efect of silver nanoparticles array [J]. ***Acta Physica Sinica***, 2018, 67(19): 197302. (in Chinese)

[8] Yao Jianquan, Di Zhigang, Jia Chunrong, et al. Photonic crystal fiber SERS sensors [J]. ***Infrared and Laser Engineering***, 2011, 40(1): 96-106. (in Chinese)

[9] Di Zhigang, Jia Chunrong, Yao Jianquan, et al. Optimization on HCPCF SERS sensor based on silver nanoparticles [J]. ***Infrared and Laser Engineering***, 2015, 44 (4): 1317-1322. (in Chinese)

[10] Cordeiro C M B, de Matos C J S, dos Santos E M, et al. Towards practicalliquid and gas sensing with photonic crystal fibers: side access to the fiber microstructure and single-mode liquid-core fiber [J]. ***Measurement Science and Technology***, 2007, 18(10): 3075-3081.

[11] Smolka S, Barth M, Benson O. Highly efficient fluorescence sensing with hollow core photonic crystal fibers [J]. ***Optics Express***, 2007, 15(20): 12783-12791.

[12] Fu Guangwei, Bi Weihong, Jin Wa. Heat transfer of fusion splicing photonic crystal fiber[J]. ***Chinese Journal of Lasers***, 2009, 36(9): 2372-2379. (in Chinese)

[13] Saleh B E A. Fundamentals of Photonics [M]. Chichester: John Wiley, 2007: 68-98.

[14] Creighton J A, Blatchford C G, Albrecht M G, et al. Plasma resonance enhancement of Raman scattering by pyridine adsorbed on silver or gold sol particles of size comparable to the excitation wavelength[J]. ***J Chem Soc***, 1979, 75: 795-798.

[15] Liu R, Zi X, Kang Y, et al. Surface-enhanced Raman scattering study of human serum on PVA Ag nanofilm prepared by using electrostatic selfassembly [J]. ***Journal of Raman Spectroscopy***, 2015, 42(2): 137-144.

[16] Di Zhigang, Yao Jianquan, Zhang Peipei, et al. Simulation and optimization of SERS effect in nano Ag substrates [J]. ***Laser & Infared***, 2011, 41(8): 850-855. (in Chinese)

[17] Zhang Yi, Shi Chao, Gu Claire. Liquid core photonic crystal fiber sensor based on surface enhanced Raman scattering [J]. ***Applied Physics Letters***, 2007, 90: 193504-193506.

[18] Richard L M. Raman Spectroscopy for Chemical Analysis [M]. New York: John Wiley & Sons, 2005: 420.